

Yellow-green emitting $\text{CaGa}_2\text{S}_4:\text{Eu}^{2+}$ phosphor: an application for enhancing the luminous flux of the white light emitting diodes

Le Thi Thuy My¹, My Hanh Nguyen Thi², Hoang Thinh Nhan³

¹Faculty of Basic Sciences, Vinh Long University of Technology Education, Vinh Long Province, Vietnam

²Faculty of Mechanical Engineering, Industrial University of Ho Chi Minh City, Ho Chi Minh City, Vietnam

³Nguyen Tat Thanh University Innovation Incubation Center, Nguyen Tat Thanh University, Ho Chi Minh City, Vietnam

Article Info

Article history:

Received Sep 10, 2022

Revised Jul 5, 2023

Accepted Jul 8, 2023

Keywords:

$\text{CaGa}_2\text{S}_4:\text{Eu}^{2+}$

Color quality

Lumen output

Mie-scattering theory

Quantum dots-WLED

ABSTRACT

The optimal spectral characteristics and photometric qualities in white-emitting light-emitting diodes (WLEDs) featuring red-emitting LEDs instead of phosphor (pc/R-WLEDs) were determined using the luminescent efficiency (LE) theory. The color quality scale (Rf) is higher than 97K for correlating color temperature (CCTs) ranging between 2700K and 6500K. We first identified genuine pc/R-WLEDs having Rf levels at 96–97, LE levels at 120–124 lm/W with CCT levels at 2969K, 4468K, 5682K, as well as 6558K with the utilization of all four-color phosphors: blues (448 nm), reddish (650 nm) LEDs, greenish (507 nm), and yellowish (586 nm). When compared to phosphorus-converted white-emitting LEDs (pc-WLEDs) and quantum dots white-emitting LEDs (QD-WLEDs), the pc/R-WLEDs, rather than the QD-WLED, would make better representatives of improved color version, notably in the reduced color temperatures, and could eventually replace current pc-WLEDs.

This is an open access article under the [CC BY-SA](https://creativecommons.org/licenses/by-sa/4.0/) license.



Corresponding Author:

My Hanh Nguyen Thi

Faculty of Mechanical Engineering, Industrial University of Ho Chi Minh City

No. 12 Nguyen Van Bao Street, Ho Chi Minh City, Vietnam

Email: nguyenthimyhanh@iuh.edu.vn

1. INTRODUCTION

The phosphorus-covered white-emitting light-emitting diodes (WLEDs), the quantum dots white-emitting LED (QD-WLED), along with the pc-WLED featuring red-LEDs in place of the phosphorus (pc/R-WLED) are the three popular types of high-efficiency hybrid white LEDs. People have always acquired ideal color rendition characteristics, natural illumination resources, as well as high efficiency. The basic color render indices (Ra) [1] and luminescent efficiency (LE) [2] are commonly applied to describe the efficiency of hybridized white-emitting LEDs. Previously, we investigated WLEDs enhancement below the constraints of the given correlating color temperatures (CCT) and color rendering indices by optimizing radiated luminescent efficiency (LER). With Ra, R9 larger than 98, CCTs adjustable phosphorus-covered/R-WLED device comprising the blue-emitting InGaN chips, the red-emitting AlGaInP sensor, as well as the green and yellow-emitting silicate phosphorus may yield LER greater than 296 lm/W over CCT value between 2700K and 6500K [3].

The blue LED-triggered quantum dots-WLEDs containing green, red, and yellow-emitting QDs were reported to have LERs at 327–371 lm/W with R9 and Ra equal to 95 under 2700K-6500K CCTs [4]. To account for the Stokes shift's waste of power, restricted luminescent efficiency is recommended (LLE). Optimizing LLE of required color rendition, many ideal hybridized white-emitting LEDs is discovered [5]–[8]. Ra, R9 of over 98 for CCTs range between 2700K and 6500 K, the CCT adjustable pc/R-WLED device containing the blue and red

chips, accompanied by phosphors in yellow as well as green might achieve LLEs at 276–309 lm/W [9]. Blue-chip-activated QD-WLEDs comprising blue CsPb(Cl_{0.1}Br_{0.9})₃, greenish CsPb(Br_{0.9}IO_{0.1})₃, yellowish CsPb(Br_{0.5}IO_{0.5})₃, as well as scarlet CsPb(Br_{0.2}IO_{0.8})₃ QDs operated achieved CCTs adjustable white-emitting lights having Ras between 96 and 97 along with LLE values between 243 and 254 lm/W from CCT values between 2700K and 6500K. As CCTs are at 2731K and 6533K, white LED genuine R/Y/C compositions can provide CCTs adjustable white-emitting lights featuring Ra values between 97 and 98, R9 values between 98 and 99, as well as Le values between 122 and 132 lm/W [10]. Ra is a regularly used metric to assess color rendition. The fact that Ra might award high evaluation compared to resources that do a poor job of rendering saturated object colors is one issue [11], [12]. To address the shortcomings of the Ra, the illuminating engineering society (IES) recently developed one dual-state mechanism [13] that includes color quality scales (Rf) and related color spectrum indices (Rg) [13], [14]. The CIE approach approved this technique [15]. The Rfs in the pc/R and QD-WLED device, along with the R/Y/C white-emitting LED compositions remained under 95 according to IES testing. As a result, their color-rendered characteristics could not reach to quality of CIE. Baslamisli and Gevers [16] found that four-phase LED devices containing colors of red, green, yellow, along with blue LEDs might achieve considerable color rendition regarding Rf at 93–94 and Ra at 95–97, as well as reasonably large LER of 299–339 lm/W and exceptional LER of 299–339 lm/W throughout a diverse CCT variety among 2800K and 6500K. At 2800K-6500K CCTs, a realistic 17-channel LED array featuring 93–97 Rfs, 100–102 Rgs, and 282–312 lm/W LERs was displayed, comprising 13 sorts of restrictive-band LEDs and four kinds of phosphorus-covered white-emitting LEDs having 93–97 Rfs, 100–102 Rgs, as well as 282–312 lm/W LERs.

It's a shame there was no information on the 17-phase LEDs set's luminous effectiveness. LLE, however, is predicated on the assumption that incoming photons are equivalent to outgoing photons. The LE enhanced simulation of CCTs adjustable pc-WLEDs was currently devised. With CCT values between 2700K and 6500K, optimum blue-chip-activated pc-WLEDs featuring yellow, green, and red-emitting phosphorus may reach 97 Rfs as well as 118–127 lm/W LEs, with a radiating efficacy (Re) at 60% for the blue-emitting chip and quantum efficacy (Qe) at 90% for the phosphorus layer. At CCTs of 3037K, 4081K, 4951K, and 6443K, these four actual PC-WLEDs featured 96–97 Rfs and 93–106 lm/W LEs have been demonstrated [17]. The development of the LE simulation of pc/R-WLEDs to analyze the optical efficiency of three variations of hybridized white-emitting LEDs is essential. Until now, no one has looked at spectrum enhancement for the CCT adjustable pc/R-WLEDs through optimizing LE using specific Rf. LE's framework of pc/R-WLED, which was established in this study, contains the Res in blue-emitting and red-emitting LEDs, and Qe in the dual-hue phosphorus layer as well. This research deeply analyzes the optical and spectrophotometric capabilities of pc/R-WLEDs, as well as the optimum spectrum properties of every colored element. In the case where Rf is at 97, to optimize the median LE with CCTs ranging between 2700K and 6500K. In addition, LE teams discussed the photometric performance of three hybridized white-emitting LEDs variations at 97 Rf. Finally, four of the most promising possibilities were demonstrated: 96–97 Rfs and 120–124 LEs when CCTs are at the following 2969K, 3955K, 5034K, as well as 6558K will be featured inside pc/R-WLEDs.

2. METHOD

2.1. Preparing CaGa₂S₄:Eu²⁺

This yellow-green-emitting CaGa₂S₄:Eu²⁺ phosphor is an indispensable part of our investigation. For the task of acquiring sheets of phosphor that yield accurate outcomes, appropriately creating the phosphor substance is very crucial. Table 1 demonstrates that CaGa₂S₄:Eu²⁺ includes 3 constituents. The creation procedure contains two firing phases. Prior to the initial phase, we mix the constituents via slurring in water, which will form a compound. Let the compound dry naturally and powderize it after. The first stage begins by firing the compound within open quartz boats under approximately 800 °C in H₂S for 1 hour, then milling the compound. The last phase involves firing the compound one more time within open quartz boats with the same time and temperature. However, this stage includes N₂ bubbling through CS₂ during the firing. Afterward, the compound is pulverized. Finally, store the mixture in a well-closed container. As expected, the results should have these optical properties discharge apex of 2.22 eV, along with an emission width (FWHM) of 0.24 eV. The UV simulated exciting efficacy should show ++ (4.88 eV), + (3.40 eV), as well as 7% by e-ray. A final note to remember is the unstable status when this phosphor is within water [18]–[20].

Table 1. Ingredients of CaGa₂S₄:Eu²⁺ phosphor composition

Ingredient	Mole %	By weight (g)
CaCO ₃	99	99
Ga ₂ O ₃	200 (of Ga)	187
Eu ₂ O ₃	1 (of Eu)	1.76

2.2. Photometric enhancement simulation

The comparative spectrum power dispersion (SPD) in the pc/R-WLED is made up of green and yellow phosphorus-covered LEDs (or pc-LEDs) controlled through a blue-emitting LED, along with red-emitting LEDs, the formula of $S_{pc/R}(\lambda)$ [21]–[23]:

$$S_{pc/R}(\lambda) = k_{pc}S_{pc}(\lambda) + k_r S(\lambda, \lambda_r, \Delta\lambda_r) \quad (1)$$

in which $S_{pc}(\lambda)$ and $S(\lambda, \lambda_r, \Delta\lambda_r)$ are the comparable SPDs in the phosphorus-covered and red-emitting LED, respectively. λ_r and $\Delta\lambda_r$ are the maximum wavelength (WL) and the full width at half maximum (FWHM) for the red-emitting LED. The ratios between pc-LED as well as red LED relative spectra, correspondingly, are k_{pc} and k_r [23]. Inside these percentage coefficients, there is just a single individual variable for the comparative SPD from pc/R-WLED (k_{pc} and k_r). $S_{pc}(\lambda)$, the comparative SPD in pc-LEDs, is calculated as (2).

$$S_{pc}(\lambda) = q_b S(\lambda, \lambda_b, \Delta\lambda_b) + q_g S(\lambda, \lambda_g, \Delta\lambda_g) + q_y S(\lambda, \lambda_y, \Delta\lambda_y) \quad (2)$$

In which $S(\lambda, \lambda_b, \Delta\lambda_b)$, $S(\lambda, \lambda_g, \Delta\lambda_g)$, and $S(\lambda, \lambda_y, \Delta\lambda_y)$ denote the comparative SPDs within the blue spectral, as well as the orange and green phosphor coating, conveyed across the phosphorus layer. The optimum WLs of blue and green-emitting LED, and orange phosphorus, accordingly, are denoted by λ_b , λ_g , and λ_y . Their FWHMs are denoted by $\Delta\lambda_b$, $\Delta\lambda_g$, and $\Delta\lambda_y$. q_b , q_g , and q_y denote the blue spectra percentage conveyed via the phosphorus film, and the green, and orange-emitting phosphors, correspondingly. We utilize the Ohno model [24] SPDs on both the red and blue-emitting LEDs. Phosphor SPDs are described simply as Gaussian function upon this photon energy level [24]. N_p is the quantity of poor-energy photons released per second in a phosphorus film made up of green/yellow phosphorus mixes. Which formula is calculated by:

$$N_p = \frac{k_{pc}q_g}{hc} \int_{\lambda} S(\lambda, \lambda_g, \Delta\lambda_g) \lambda d\lambda + \frac{k_{pc}q_y}{hc} \int_{\lambda} S(\lambda, \lambda_y, \Delta\lambda_y) \lambda d\lambda \quad (3)$$

the quantity of the potent-power blueish photons occluded via the phosphorus layers in green/yellow every second, N_{ab} as shown in:

$$N_{ab} = \frac{q_{ab}}{hc} \int_{\lambda} S(\lambda, \lambda_b, \Delta\lambda_b) \lambda d\lambda \quad (4)$$

the occluded blue illumination fraction, Planck's constant [25], and lighting speed, accordingly, are denoted by q_{ab} , h , and c . Because the absorbed percentage, q_{ab} , for the phosphor sheet in green/yellow will be specified as N_p/N_{ab} , the following formula may be used to compute it:

$$q_{ab} = \frac{k_{pc}q_g \int_{\lambda} S(\lambda, \lambda_g, \Delta\lambda_g) \lambda d\lambda + k_{pc}q_y \int_{\lambda} S(\lambda, \lambda_y, \Delta\lambda_y) \lambda d\lambda}{Q_e \int_{\lambda} S(\lambda, \lambda_b, \Delta\lambda_b) \lambda d\lambda} \quad (5)$$

the blue LED's radiant efficiency, $R_{e,b}$, is computed as:

$$R_{e,b} = \frac{1}{P_{in,b}} \int_{\lambda} (k_{pc}q_b + q_{ab}) S(\lambda, \lambda_b, \Delta\lambda_b) d\lambda \quad (6)$$

the radiant efficacy for the red-emitting LED, will be as:

$$R_{e,r} = \frac{1}{P_{in,r}} \int_{\lambda} k_r S(\lambda, \lambda_r, \Delta\lambda_r) d\lambda \quad (7)$$

the standard source energy of blue and red-emitting LEDs, correspondingly, is denoted by $P_{in, b}$ and $P_{in, r}$. As a result, a pc/R-WLED device's LE value may be computed by adding the radiant efficacy from blue as well as red-emitting LED devices, along with the quantum efficacy for the green/yellow phosphorus layer [26].

$$LE = \frac{683}{(P_{in,b} + P_{in,r})} \int_{\lambda} V(\lambda) S_{pc/R}(\lambda) d\lambda = \frac{683 \int_{\lambda} V(\lambda) S_{pc/R}(\lambda) d\lambda}{\frac{1}{R_{e,b}} \int_{\lambda} (k_{pc}q_b + q_{ab}) S(\lambda, \lambda_b, \Delta\lambda_b) d\lambda + \frac{1}{R_{e,r}} \int_{\lambda} k_r S(\lambda, \lambda_r, \Delta\lambda_r) d\lambda} \quad (8)$$

In which $V(\lambda)$ is the photopic luminescent efficacy function of the 1988 CIE [27]. The median LE value for a pc/R-WLED device with adjustable CCT featuring blue as well as red-emitting LED devices ($R_{e,b}$ and $R_{e,r}$ equal to 60%) along with the phosphorus film in green/yellow (Q_e equal to 90%) when R_f is at least 97 will be determined as:

$$F = \sum_{j=1}^8 LE_j(k_{r,j}\lambda_b, \lambda_g, \lambda_y, \lambda_r, \Delta\lambda_b, \Delta\lambda_g, \Delta\lambda_y, \Delta\lambda_r) \tag{9}$$

(For $R_f \geq 97, D_{uv} = 0$)

2700K, 3000K, 3500K, 4000K, 4500K, 5000K, 5700K, and 6500K of CCTs are represented by the subscripts $j = 1, 2, 3, 4, 5, 6, 7,$ and 8 . Mixed-type WLEDs' chromaticity was forced to lay on the Planckian axis with a CCT value beneath 5000K, and the daylight locus with a CCT value over 5000K the chromatic disparity between the 2 mentioned cases in the CIE 1960 UV chromatic chart (D_{uv}) would be 0. Under disparate maximum WL values with FWHM values for the LED device as well as phosphor, a $D_{uv} = 0$ limit is used to prevent going outside the white-light source's chromatic sensitivity quadrangles.

During the optimizing process, the selected WLs for the pc/R WLED were 450 and 470 nm of the blue-emitting LED, 490 and 550 nm of the greenish phosphorus, 550 and 600 nm of the yellow-emitting phosphorus, along with 600 and 650 nm in the case of the red-emitting LED. Furthermore, the FWHMs for blue LEDs range from 25 to 35 nm, for green and yellow-emitting phosphors from 70 to 120 nm, and for red LEDs from 20 to 30 nm. The viable vectors are located upon the hypersurface including 9 dimensionalities when the 12-dimensional factor gap is subjected to three color-combining restrictions, hence the goal value F excludes the parameters comprising $k_{pc}, q_b, q_g,$ and q_y . As a result, the enhancement issue boils down to determining the optimum of the goal values (F). As it can examine a large number of alternatives, without a starting resolution, is effective in complex situations, and could be easily altered to approximate the Pareto ideal set, a rapid Pareto genetics method is employed in optimization. The recreation of phosphorus layers from the MCW-LED device are through films of silicon will be done with software LightTools 9.0 as well as the Monte Carlo process.

The recreation is divided into two phases: the first phase defines, then constructs MCW-LED formations along with light attributes. The last phase regulates phosphor's light influences via shifting $CaGa_2S_4:Eu^{2+}$ content. Thorough examination is needed to gauge the influence from $YAG:Ce^{3+}$ as well as $CaGa_2S_4:Eu^{2+}$ phosphorus compound upon the MCW-LED lights output. It is necessary to understand the nature of two-sheet distant phosphorus, which is considered two blends having median CCT levels measured at 3000K, 4000K, and 5000K. The said device's illumination that possesses one conformal phosphorus mixture, as well as an 8500K mean CCT, are depicted in detail in Figure 1. The simulation for devices lacking $CaGa_2S_4:Eu^{2+}$ would be suitable as well. The reflector's floor size, width, and outer layer length are reported as 8, 2.07, and 9.85 mm, accordingly. The said phosphorus blend will be daubed on nine 0.08 mm thick chips. 1.14 mm² base region area and 0.15 mm width connect each LED's chip to the reflector cavity. All blue-emitting chips yield a radiating output measured at 1.16 W accompanied by one 453 nm peak wavelength range.

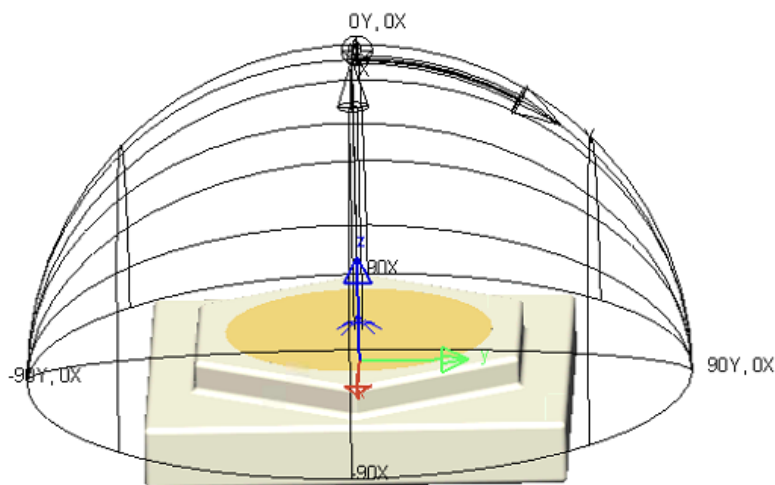


Figure 1. WLED device recreated

3. RESULTS AND DISCUSSION

The inversed correlation among several contents for $\text{CaGa}_2\text{S}_4:\text{Eu}^{2+}$ as well as yellowish $\text{YAG}:\text{Ce}^{3+}$ phosphors is displayed by Figure 2. Such adjustment has two aspects: to keep the median CCT's value, and to alter the absorptivity along with dispersal for the WLED device containing a pair of phosphor sheets, influencing WLED's hue quality along with light flux performance. The hue output in the device will be then altered via the $\text{CaGa}_2\text{S}_4:\text{Eu}^{2+}$ concentration chosen. When the $\text{CaGa}_2\text{S}_4:\text{Eu}^{2+}$ content surged (2%-20% Wt.), the $\text{YAG}:\text{Ce}^{3+}$ content diminished, which retained the mean values of CCT. Devices featuring hue temperatures from 5600-8500K will also be subjected to this rule.

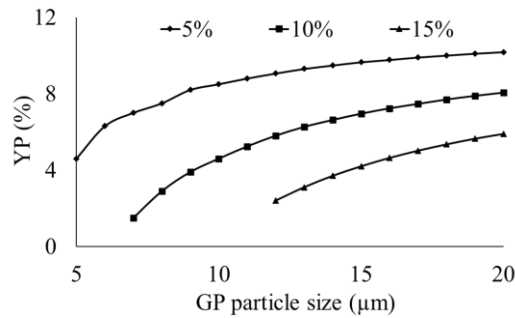


Figure 2. Retaining median CCT values via altering phosphor contents

The illustration in Figure 3 is the green phosphorus $\text{CaGa}_2\text{S}_4:\text{Eu}^{2+}$ concentration's influence on WLED's transmittance spectrum. Assessing the demands of production will help us pick a suitable option. High chroma consistency in WLED apparatuses will yield minimal penalty for lumen. White illumination occurs as a result of the spectrum area's composition, which exhibit 5600-8500K spectra, accordingly. The intensity is inflated alongside the $\text{CaGa}_2\text{S}_4:\text{Eu}^{2+}$ content for specific zones within the spectrum for illumination: 420-480 nm along with 500-640 nm. Superior lumen is observed through the double-bar discharge spectrum. Likewise, the increase of blue-light scattering in WLEDs implies that dispersion within the phosphorous sheet as well as WLED device also rises, favoring chroma consistency. The chroma balance for the remote phosphor setting under considerable heat level may prove challenging for controlling. Our assessment found that $\text{CaGa}_2\text{S}_4:\text{Eu}^{2+}$, at 5600K along with 8500K, could augment WLED's hue quality. In the research, the output for the generated luminous flux from the double-sheet phosphorus setting was investigated more extensively. The results from Figure 4 show that as the concentration of $\text{CaGa}_2\text{S}_4:\text{Eu}^{2+}$ grew from 2% wt to 5% wt, the luminous flux increased substantially, reaching 20% by weight. The hue deviance immensely fell alongside the phosphor $\text{CaGa}_2\text{S}_4:\text{Eu}^{2+}$ content, as shown with the CCT levels from

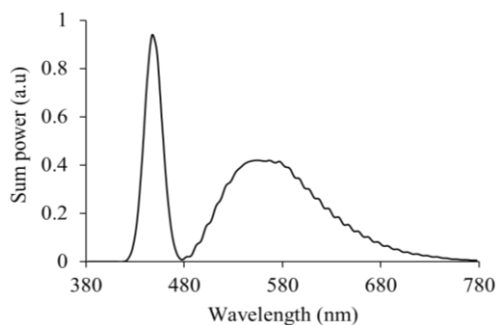


Figure 3. $\text{CaGa}_2\text{S}_4:\text{Eu}^{2+}$ concentration functions as WLEDs emitting spectrum measured at 6000K

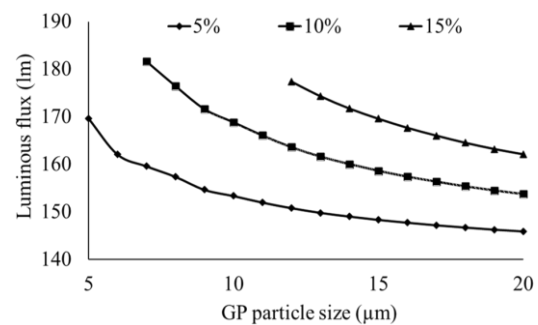


Figure 4. $\text{CaGa}_2\text{S}_4:\text{Eu}^{2+}$ content correlating with lumen in WLED

Figure 5 the red phosphor layer's absorption is the inducement for this event. When the $\text{CaGa}_2\text{S}_4:\text{Eu}^{2+}$ phosphor absorbed the blue ray made via the chip in LED which then gets replaced by the green color. The yellow illumination would also be absorbed through the $\text{CaGa}_2\text{S}_4:\text{Eu}^{2+}$ granules from the said chip with the

blue-emitted light. The blue absorption, however, is the strongest, a result of the absorbtivity from the substance. By adding $\text{CaGa}_2\text{S}_4:\text{Eu}^{2+}$, the greenish content within WLEDs rises, augmenting hue consistency. Hue consistency would be highly vital. As the hue consistency index surges, the cost of WLED devices will surge as well. However, the low cost from using $\text{CaGa}_2\text{S}_4:\text{Eu}^{2+}$ is an advantage. $\text{CaGa}_2\text{S}_4:\text{Eu}^{2+}$ has the potential for popular use.

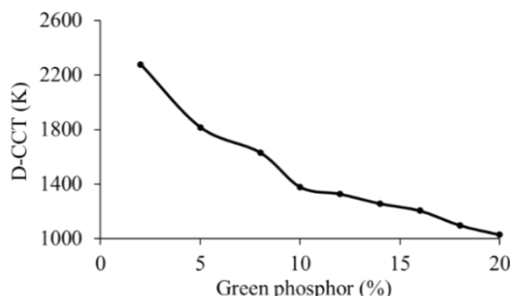


Figure 5. $\text{CaGa}_2\text{S}_4:\text{Eu}^{2+}$ content correlating with hue deviance in WLED

The task of gauging hue output in WLED would require many factors, besides the hue consistency. The hue aspects cannot be considered as good with high color homogeneity index. Consequently, recent studies utilized CRI along with CQS. With CRI as gauging factor, an illuminated item will show its actual hue. The immoderate abundance in green illumination among the dominant shades (blue, yellow, green) results in colour disparity, affecting color quality in WLED, causing deficit for the hue fidelity. Figures 6 and 7 demonstrates the tiny decline of CRI and CQS with the remote phosphor $\text{CaGa}_2\text{S}_4:\text{Eu}^{2+}$ layer, respectively. Besides the blue light, the $\text{CaGa}_2\text{S}_4:\text{Eu}^{2+}$ particles consumed the yellow light originated in the LED’s chip. And once again, the blue-emitting light absorption is excessively active thanks to the absorbtivity from the substance. CRI and CQS fall considerably if $\text{CaGa}_2\text{S}_4:\text{Eu}^{2+}$ content becomes preponderant over 10% wt., caused by the sunstantial hue dissipation when green turns dominant. Gauging a proper concentration for $\text{CaGa}_2\text{S}_4:\text{Eu}^{2+}$ will be a vital task.

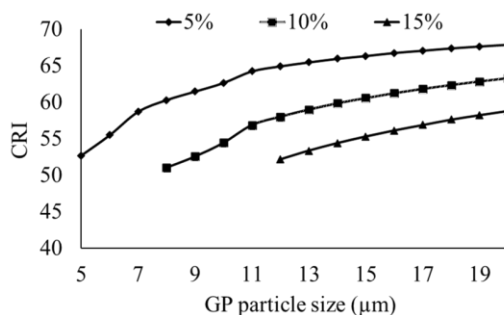


Figure 6. $\text{CaGa}_2\text{S}_4:\text{Eu}^{2+}$ content correlating with CRI in WLED

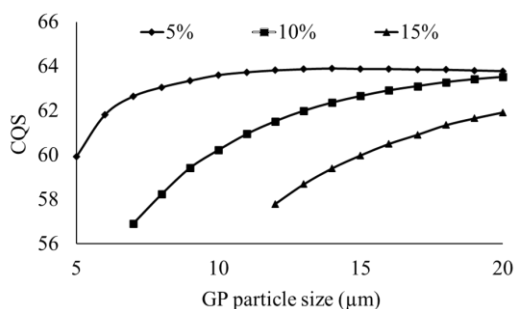


Figure 7. $\text{CaGa}_2\text{S}_4:\text{Eu}^{2+}$ content correlating with CQS in WLED




4. CONCLUSION

The attributes in the phosphor arrangement with double sheets are studied using $\text{CaGa}_2\text{S}_4:\text{Eu}^{2+}$ green phosphorus. The study found that $\text{CaGa}_2\text{S}_4:\text{Eu}^{2+}$ would augment hue uniformity through Monte Carlo computer recreations, being natural to WLED devices featured hue temperatures below 5600K and over 8500K. The study results were able to attain the aim of boosting color quality as well as lumen, due to the distant arrangement for phosphor. Regardless, CRI and CQS will yield a minor downside. The CRI and CQS noticeably waned in case the $\text{CaGa}_2\text{S}_4:\text{Eu}^{2+}$ concentration rises excessively. Hence, an appropriate content of the phosphor must be decided by considering the aims of manufacturers. The paper has yielded agitatedly valuable information when it comes to realizing superior color consistency along with luminous flux for WLED devices.




REFERENCES

- [1] B. Fan, H. Wu, Y. Zhao, Y. Xian, and G. Wang, "Study of phosphor thermal-isolated packaging technologies for high-power white light-emitting diodes," *IEEE Photonics Technology Letters*, vol. 19, no. 15, pp. 1121–1123, Aug. 2007, doi: 10.1109/LPT.2007.901098.
- [2] J. S. Li, Y. Tang, Z. T. Li, J. X. Chen, X. R. Ding, and B. H. Yu, "Precise optical modeling of phosphor-converted LEDs with arbitrary concentration and thickness using bidirectional scattering distribution function," *IEEE Photonics Journal*, vol. 10, no. 5, pp. 1–17, Oct. 2018, doi: 10.1109/JPHOT.2018.2866864.
- [3] F. Brusola, I. Tortajada, I. Lengua, B. Jordá, and G. Peris-Fajarnés, "Parametric effects by using the strip-pair comparison method around red CIE color center," *Optics Express*, vol. 28, no. 14, p. 19966, Jul. 2020, doi: 10.1364/oe.395291.
- [4] B. Zhao, Q. Xu, and M. R. Luo, "Color difference evaluation for wide-color-gamut displays," *Journal of the Optical Society of America A*, vol. 37, no. 8, p. 1257, Aug. 2020, doi: 10.1364/josaa.394132.
- [5] J. O. Kim, H. S. Jo, and U. C. Ryu, "Improving CRI and scotopic-to-photopic ratio simultaneously by spectral combinations of cct-tunable led lighting composed of multi-chip leds," *Current Optics and Photonics*, vol. 4, no. 3, pp. 247–252, 2020, doi: 10.3807/COPP.2020.4.3.247.
- [6] N. A. Mica *et al.*, "Triple-cation perovskite solar cells for visible light communications," *Photonics Research*, vol. 8, no. 8, p. A16, Aug. 2020, doi: 10.1364/prj.393647.
- [7] P. Kaur, Kriti, Rahul, S. Kaur, A. Kandasami, and D. P. Singh, "Synchrotron-based VUV excitation-induced ultrahigh quality cool white light luminescence from Sm-doped ZnO," *Optics Letters*, vol. 45, no. 12, p. 3349, Jun. 2020, doi: 10.1364/ol.395393.
- [8] A. Ali *et al.*, "Blue-laser-diode-based high CRI lighting and high-speed visible light communication using narrowband green-/red-emitting composite phosphor film," *Applied Optics*, vol. 59, no. 17, p. 5197, 2020, doi: 10.1364/ao.392340.
- [9] B. K. Tsai, C. C. Cooksey, D. W. Allen, C. C. White, E. Byrd, and D. Jacobs, "Exposure study on UV-induced degradation of PTFE and ceramic optical diffusers," *Applied Optics*, vol. 58, no. 5, p. 1215, Feb. 2019, doi: 10.1364/ao.58.001215.
- [10] Y. Wang, G. Xu, S. Xiong, and G. Wu, "Large-field step-structure surface measurement using a femtosecond laser," *Optics Express*, vol. 28, no. 15, p. 22946, 2020, doi: 10.1364/oe.398400.
- [11] M. A. Elkaram, M. H. Aly, H. M. A. Kader, and M. M. Elsherbini, "LED nonlinearity mitigation in LACO-OFDM optical communications based on adaptive predistortion and postdistortion techniques," *Applied Optics*, vol. 60, no. 24, p. 7279, Aug. 2021, doi: 10.1364/ao.432364.
- [12] H. Yuce, T. Guner, S. Balci, and M. M. Demir, "Phosphor-based white LED by various glassy particles: control over luminous efficiency," *Optics Letters*, vol. 44, no. 3, p. 479, 2019, doi: 10.1364/ol.44.000479.
- [13] H. Q. T. Bui *et al.*, "High-performance nanowire ultraviolet light-emitting diodes with potassium hydroxide and ammonium sulfide surface passivation," *Applied Optics*, vol. 59, no. 24, p. 7352, Aug. 2020, doi: 10.1364/ao.400877.
- [14] T. W. Kang *et al.*, "Enhancement of the optical properties of CsPbBr₃ perovskite nanocrystals using three different solvents," *Optics Letters*, vol. 45, no. 18, p. 4972, Sep. 2020, doi: 10.1364/OL.401058.
- [15] S. Keshri *et al.*, "Stacked volume holographic gratings for extending the operational wavelength range in LED and solar applications," *Applied Optics*, vol. 59, no. 8, p. 2569, Mar. 2020, doi: 10.1364/AO.383577.
- [16] A. S. Baslamisli and T. Gevers, "Invariant descriptors for intrinsic reflectance optimization," *Journal of the Optical Society of America A*, vol. 38, no. 6, p. 887, Jun. 2021, doi: 10.1364/JOSAA.414682.
- [17] G. Granet and J. Bischoff, "Matched coordinates for the analysis of 1D gratings," *Journal of the Optical Society of America A*, vol. 38, no. 6, p. 790, Jun. 2021, doi: 10.1364/JOSAA.422374.
- [18] Q. Xu, B. Zhao, G. Cui, and M. R. Luo, "Testing uniform colour spaces using colour differences of a wide colour gamut," *Optics Express*, vol. 29, no. 5, p. 7778, Mar. 2021, doi: 10.1364/OE.413985.
- [19] A. Alexeev, J.-P. M. G. Linnartz, K. Arulandu, and X. Deng, "Characterization of dynamic distortion in LED light output for optical wireless communications," *Photonics Research*, vol. 9, no. 6, p. 916, Jun. 2021, doi: 10.1364/PRJ.416269.
- [20] R. Fan, S. Fang, C. Liang, Z. Liang, and H. Zhong, "Controllable one-step doping synthesis for the white-light emission of cesium copper iodide perovskites," *Photonics Research*, vol. 9, no. 5, p. 694, May 2021, doi: 10.1364/PRJ.415015.
- [21] X. Xi *et al.*, "Chip-level Ce:GdYAG ceramic phosphors with excellent chromaticity parameters for high-brightness white LED device," *Optics Express*, vol. 29, no. 8, p. 11938, Apr. 2021, doi: 10.1364/OE.416486.
- [22] I. Fujieda, Y. Tsutsumi, and S. Matsuda, "Spectral study on utilizing ambient light with luminescent materials for display applications," *Optics Express*, vol. 29, no. 5, p. 6691, Mar. 2021, doi: 10.1364/oe.418869.
- [23] Y. Wang *et al.*, "Tunable white light emission of an anti-ultraviolet rare-earth polysiloxane phosphors based on near UV chips," *Optics Express*, vol. 29, no. 6, p. 8997, Mar. 2021, doi: 10.1364/OE.410154.
- [24] J. R. Beattie and F. W. L. Esmonde-White, "Exploration of principal component analysis: Deriving principal component analysis visually using spectra," *Applied Spectroscopy*, vol. 75, no. 4, pp. 361–375, Apr. 2021, doi: 10.1177/0003702820987847.
- [25] M. Chlipala and T. Kozacki, "Color LED DMD holographic display with high resolution across large depth," *Optics Letters*, vol. 44, no. 17, p. 4255, Sep. 2019, doi: 10.1364/OL.44.004255.
- [26] K. J. Francis, Y. E. Boink, M. Dantuma, M. K. A. Singh, S. Manohar, and W. Steenbergen, "Tomographic imaging with an ultrasound and LED-based photoacoustic system," *Biomedical Optics Express*, vol. 11, no. 4, p. 2152, Apr. 2020, doi: 10.1364/BOE.384548.
- [27] S.-H. Lin *et al.*, "Enhanced external quantum efficiencies of AlGaIn-based deep-UV LEDs using reflective passivation layer," *Optics Express*, vol. 29, no. 23, p. 37835, Nov. 2021, doi: 10.1364/OE.441389.




BIOGRAPHIES OF AUTHORS

Le Thi Thuy My    received the Master degree in physics from Can Tho University, Vietnam. She is working as a lecturer at the Faculty of Basic Sciences, Vinh Long University of Technology Education, Vietnam. Her research interests focus on developing the patterned substrate with micro- and nano-scale to apply for physical and chemical devices such as solar cells, OLED, photoanode, and theory physics. She can be contacted at email: mylth@vlute.edu.vn.



My Hanh Nguyen Thi    received a Bachelor of Physics from An Giang University, VietNam, Master of Theoretical Physics And Mathematical Physics, Hanoi National University of Education, VietNam. Currently, she is a lecturer at the Faculty of Mechanical Engineering, Industrial University of Ho Chi Minh City, Viet Nam. Her research interests are theoretical physics and mathematical physics. She can be contacted at email: nguyenthimyhanh@iuh.edu.vn.



Hoang Thinh Nhan    received his Engineer Diploma in Mechanical Engineering (Industrial Machines, Equipment and Process) from Ufa State Petroleum Technology University (USPTU), Russia, in 2003 and Ph.D. Degree in Mechanical Engineering from USPTU in 2006. He is currently working as Deputy Director of Center of Innovation and Business Incubation in the Nguyen Tat Thanh University, Ho Chi Minh City, Vietnam. His research interests include renewable energy, optimization techniques, hydraulic and pneumatic systems, and offshore engineering. He can be contacted at email: htnhan@ntt.edu.vn.